Annals of Phytomedicine 12(1): 251-258, 2023

DOI: http://dx.doi.org/10.54085/ap.2023.12.1.27

Annals of Phytomedicine: An International Journal
http://www.ukaazpublications.com/publications/index.php

Print ISSN : 2278-9839 Online ISSN : 2393-9885

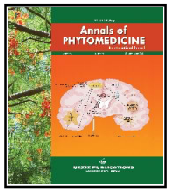

Original Article : Open Access

Interaction between anti-COVID compounds across spike protein subunits influences their inhibition potential

Medhat Farag◆, Aslam Pathan* and Nawaf Aldoij**

Department of Basic Medical Sciences (Biochemistry), College of Medicine, Shaqra University, Saudi Arabia
** Department of Basic Medical Sciences (Pharmacology), College of Medicine, Shaqra University, Saudi Arabia*
*** Undergraduate Student, College of Medicine, Shaqra University, Saudi Arabia*

Article Info

Article history
Received 10 February 2023
Revised 28 March 2023
Accepted 29 March 2023
Published Online 30 June-2023

Keywords
COVID-19
Spike protein
Jujuboside B
Glycyrrhizin
Vasicine

Abstract

The primary role of the Spike protein is to initiate the virus infection process. The mechanism involves a structural transition of the Spike protein that facilitates the rupture of the host membrane followed by penetration of the virus into the host cell. The trimeric organization of the Spike protein plays an important role in this process. Here, we take 10 bioactive plant products molecular docked on Spike protein by AutoDock Vina software and then perform 20 ns molecular dynamics simulation using the Gromacs software. We estimate the ligand interaction and flexibility of the Spike protein by taking the trimer together as an oligomeric unit and separately by enforcing the periodic boundary condition with a triclinic solvent box. We find that affinity is not the only determinant for potential inhibitory action, but may improve if the binding site spans across the three monomers in the trimer. The molecular dynamics simulation suggests that reduction in the fluctuation is maximum when the ligand binding site spans the three subunits. Since the function of the Spike protein is intimately involved with structural transition, we suggest the inhibitory potential of the ligands maximizes when their interaction is spread across each subunit.

1. Introduction

The COVID-19 cases are in wane after reaching a high around January 2022. This was after the spread of the Omicron variant of the SARS-CoV-2 virus (https://www.worldometers.info/coronavirus/; date: March 3, 2023). It was observed that vaccinated individuals when analyzed for viral load post-infection and recovery from Delta and Omicron variants had decreased morbidity and mortality, while for both vaccinated and unvaccinated individuals, it had a marginal effect on transmissibility with respect to the Omicron variant (Woodbridge *et al*., 2022). Thus, the chance of SARS-CoV-2 spreading to individuals remains undiminished through the emergence of new strains in near future. The development of new antiviral agents would thus help to protect against the persistent viral threat, especially if such a strain has increased lethality.

The effort to create new vaccines continues (World Health Organization Vaccine Tracker; https://www.who.int/publications/m/item/draft-landscape-of-covid-19-candidate-vaccines) with the aim to prevent infection as well as morbidity. These are guided by new ideas on how to facilitate their widespread administration (Focosi *et al*., 2023). Recently, nasal vaccines is one of the alternate approaches being promoted in the same direction (Chavda *et al*., 2023). However, immunocompromised persons are unlikely to respond robustly to vaccination, and new immune-escape variants and their spread may render even immune-competent persons with higher rates of vaccine failure (Tao *et al*., 2021). Ritonavir-boosted nirmatrelvir (Paxlovid), molnupiravir, and high-titer COVID-19 convalescent plasma are some of the antivirals currently in the market with Emergency Use Authorization from the US-FDA for use in certain patients for COVID-19 treatment. Anti-SARS-CoV-2 monoclonal antibodies, Tixagevimab 300 mg plus Cilgavimab 300 mg (Evusheld) also have emergency use approvals for SARS-CoV-2 pre-exposure prophylaxis in certain patients. General purpose antiviral thus remains to be developed for COVID-19 to mitigate the need of the market.

The use of traditional medicine for protection against COVID-19 has been in focus for its natural origin and benign use. This can be gauged from the 156 instances of the clinical trial on herbal or traditional medicine reported at the Clinical Tracker site (https://www. clinicaltrials.gov/ct2/results/details?cond=COVID-19+AND+%22COVID-19%22&term=traditional+OR+herbal). This is about 1.77% of the total number of clinical trials recorded for COVID-19. The fraction of cases is low and more work is needed in the area. Bioactive compounds bearing medicinal properties are typically minor components in plant and animal extracts. They need to be purified to explore in further detail before their use and general deployment for human health. Currently, for COVID-19, traditional medicines are primarily used for adjuvant therapy to boost immunity against infection and accelerate post-COVID recovery. In specific instances, the herbal extract has also been effective as an antiviral agent against COVID-19 (Sarkar *et al*., 2022).

Corresponding author: Dr. Medhat Farag
Professor, Department of Basic Medical Sciences (Biochemistry), College of Medicine, Shaqra University, Saudi Arabia
E-mail: m.farag@su.edu.sa
Tel.: +966-532962912

In this paper, we follow up on the study of ten natural plant active constituents; namely, Caffeine (Compound Identifier (CID) 2519), Curcumin (CID 969516), Glycyrrhizin (CID 14982), Jujuboside B (CID 24721031), Glucolepidiin (CID 656547), Linoleic acid (CID 5280450), Kaempferol (CID 5280863), Malvone A (CID 135542082), Allantoin (CID 204), Vasicine (CID 72610), from *Coffea arabica, Curcuma longa, Glycyrrhiza glabra, Zizyphus vulgaris, Sisymbrium irio, Borago officinalis, Althaea officinalis, Malva sylvestris, Cordia latifolia,* and *Adhatoda vasica,* respectively. The compounds are known to have immunomodulatory, anti-inflammatory, antioxidant, and antiviral properties. Caffeine is a strong antioxidant (Hall *et al*., 2015), while curcumin has anti-inflammatory properties (Chainani *et al*., 2003). Glycyrrhizin antiviral properties have been demonstrated *in vitro* on SARS-CoV-2 (Luo *et al*., 2020). Jujuboside B has anticoagulation, antirestenosis activity (Seo *et al*., 2013), antiasthmatic potential (Nanave *et al*, 2019), and the ability to reduce vascular tension (Zhao *et al*., 2016). Glucolepidiin acts like a prodrug in its antimicrobial properties (Romeo *et al*., 2018). Linoleic acid is an essential fatty acid useful as a precursor molecule for the synthesis of compounds important for good health (Jandacek *et al*., 2017). Kaempferol participates in oxidation, inflammation, tumor, and virus regulation activities (Devi *et al*., 2015). Malvone A activity is not well understood, but its extract from *Malva sylvestris* has antioxidant, anti-inflammatory, and antimicrobial activity (Mousavi *et al*., 2021). Allantoin has immunomodulatory activity and promotes wound healing (Araujo *et al*., 2010). Vasicine has antioxidant, anti-inflammatory, and bronchodilatory properties (Gulati *et al*, 2016). We have already studied the binding affinity of the above-mentioned molecules to the Spike protein of SARS-CoV-2 using molecular docking (Farag *et al*., 2022). However, the affinity values may not necessarily translate to the expected pharmacologic inhibition, especially when the protein is large with a quaternary structure as in the case of the Spike protein. Therefore, we perform molecular dynamics (MD) study of the Spike receptor and the various ligand bound-complexes to understand how the affinity may bring change in the molecule function by ligand interaction stabilizing the trimeric structure. Since the structural transition of the Spike protein majorly determines the infection efficiency of the SARS-CoV-2, the restriction of conformation has implications for host receptor attachment, cell penetration, and the cell-to-cell spread of the virus (Pal *et al*., 2021).

2. Materials and Methods

2.1 The Spike protein complex

The trimeric structure coordinates for the SARS-CoV-2 Spike protein were obtained from the Research Collaboratory for Structural Bioinformatics (RCSB) (https://www.rcsb.org) using Protein Data Bank (PDB) identifier (ID):6VXX (Walls *et al.*, 2020). The structure corresponds to the ectodomain of the Spike protein resembling its prefusion state. The Autodock Tools (https://autodocksuite. scripps. edu/adt/) was used to save the receptor and ligand coordinates in the pdbqt format, and the ligand binding site was calculated byAutodock Vina (Trott *et al*., 2010). Further details on the method can be obtained from the published study (Farag *et al*, 2022).

2.2 Molecular dynamics simulation

The MD simulations were performed with GROMACS version 2021.4 (Abrahm *et al*., 2015) using the CHARMM 36 force field (Huang *et al*., 2013). The receptor alone was simulated at first. The trimeric Spike structure was placed in a triclinic box with its centroid coinciding with the box center and solvated with water (Figure 1A). The size of the box was made such that there was a minimum of 20 Å distance between the edge of the molecule and the box. Na^+ and Cl^- ions were added randomly to the box replacing water molecules such that the system was neutralized and the final concentration of NaCl reached 0.1M. Periodic boundary conditions were employed for the systems in all three directions. The nonbonded interactions were accounted for using the Verlet list and we enforced short-range electrostatic and as well as van der Waals cutoff at 1.2 Å. The long-range interactions were calculated using the particle mesh Ewald (PME). The energy minimization was performed using the steepest descent method with a step size of 0.01 kJ mol^{-1} until the maximum force in the system reached below 1000 kJ mol^{-1} nm^{-1}.The NVT equilibration was performed at 300 K for 100 ps with no pressure coupling (Bussi *et al*., 2007). This was followed by NPT equilibration for 100 ps at 300 K. The parameters remained the same as in the previous step except for the addition of isotropic pressure coupling to a Parinello-Rahman barostat at 1 bar pressure with a time constant of 2 ps (Parrinello *et al.*, 1981). Thereafter, unconstrained MD was performed with the same parameters used in NPT equilibration, without the scaling of reference coordinates. The simulation time was 20 ns and the frames were saved every 100 ps, yielding 201 frames for analysis.

The MD simulation of the Spike-ligand complex was performed the same way. However, since the ligand parameters were not originally present in the CHARMM36 library, they were prepared separately using the protocols suggested in the GROMACS software tutorial (http://www.mdtutorials.com/gmx/complex/). The parameter assignment in each case was done through the CGenFF portal (https://cgenff.umaryland.edu/) (Vanommeslaeghe *et al*., 2012; Vanommeslaeghe *et al*., 2012)

The simulation of the pseudo-separated Spike trimer and all the Spike-ligand complexes was done using the same protocols as described above. The only difference in the pseudo-separated Spike trimer was the placement of the Spike molecule/Spike-ligand complex in the box (Figure 1B). Here, we put the molecule/complex centroid at 0,0,0 coordinate coinciding with one of the vertices of the triclinic box. Since PBC conditions were deployed in all three directions of the Cartesian frame, these caused each monomer chain of the molecule to translate across the periodic boundary in the simulation system.

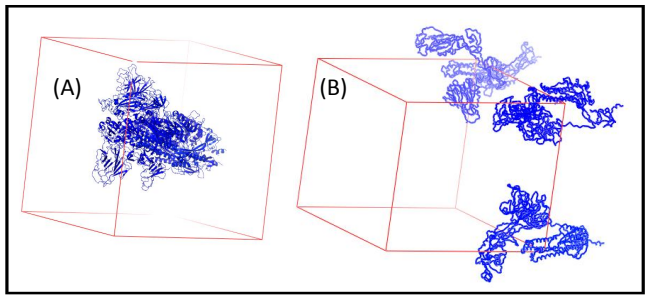

Figure 1: Placement of the Spike protein in the simulation box. (A). The center of the triclinic box and the centroid of the Spike protein timer coincides. (B). The centroid of the Spike was transformed to the origin (0,0,0) such that it coincides with one of

the vertexes of the triclinic box. There after, on the application of the periodic boundary condition (PBC), the trimer is translated as shown in the right figure. The energies are calculated by translating the coordinates inside the box. Because the coordinates are artificially translated using the PBC condition, it has been called a pseudo.

To estimate the ligand binding affinity, the "lie" utility in the GROMACS software was used. This is a free energy estimate based on an energy analysis from the nonbonded energies: Coulomb Short Range (Ligand-Protein) and Lennard Jones Short Range (Ligand-Protein). For this calculation, the "energygrps" were defined in the molecular dynamics parameter file for the ligand and the protein. Thereafter, the average values of the nonbonded energies were extracted from the trajectory using the "energy" utility of GROMACS and passed on for the affinity calculation using the "lie" utility. The same calculation was performed on the trajectory from the box-centered, and the PBC-translated Spike molecule. The variation of the energies between different ligands, structural flexibilities, and fluctuations was studied for both the original and the pseudo system.

3. Results

The effectiveness of the inhibitory activity of any ligand is typically estimated from its affinity value. A rigid-docking search allows us to do a global search of the potential site of interaction, but its validity remains unconfirmed till a molecular dynamics simulation is run with the ligand-bound complex to test if the attachment has remained stable. In the case of the ligands studied in this work, all were found to be stable both at the rigid-body docking stage and the follow-up molecular dynamics simulation. Several ligand-binding features were revealed during the detailed analysis of the results.

3.1 Correlation of binding affinity and other parameters

The rigid-body docking results revealed several interesting trends which showed that the molecular weight of the ligands correlated well (coefficient: – 0.92) with its affinity (Aff_{dock}) to the Spike protein. The affinity also correlated well (coefficient: – 0.85) with the number of hydrogen bond donors, it was also good (coefficient: – 0.90) against the number of acceptors in these molecules.This implies that the number of hydrogen bond donors and acceptors increases in the set of molecules being studied in this work proportionately according to the molecular weight of the compounds.

The correlation of the affinity calculated from the molecular dynamics simulation (Aff_{MD}) is lower than (Aff_{dock}) for each of the parameters above. For molecular weight, the correlation is reduced to – 0.60, and for hydrogen bond donors (– 0.64) and acceptors (– 0.63). It is also worthwhile to note that although the correlation between the ligand affinities calculated in the normal MD setup (Aff_{MD}) and pseudo setup (Aff_{pseudo}) is 0.60; the correlation for the latter with hydrogen bond donors is increased to (– 0.79) and acceptors (– 0.65). The difference possibly arises out of the long-range contributions made by the Coulombic force to the ligand affinity.

3.2 Comparison of affinity values

When we look at the affinity values (Table 1) obtained using Autodock Vina (Aff_{dock}) to those from the "lie" calculations (Aff_{MD}/Aff_{pseudo}) using CHARMM36 forcefield, the maximum values are comparable, but the minimum values have a significant difference, sometimes the magnitude being quite large. For example, Jujuboside B affinity (Aff_{MD}) is showing the kcal/mole value of – 25.5, compared to – 11.6 obtained from Autodock Vina. Since Autodock Vina does not use partial atomic charge in its calculations, the electrostatic component is likely under represented in the ligand affinity estimated. Besides, the higher number of hydrogen bond donors and acceptors ensures that the total contribution of the Coulombic force is likely to be larger and nonlinear in proportion due to its long-range nature. The highest deviating values are for Jujuboside, Curcumin, and Glucolepidiin. These can be assessed better by looking at the profile of interactions (next section), for better insight into its binding behavior at the site of interaction.

3.3 Ligand interaction with subunits

The binding site of the ligand when at the interface of the trimer is likely to have the maximum efficacy in inhibiting the activity, as the Spike function involves a structural transition that involves synchronized movement among the trimer as evident from the post-fusion helix-bundle structure of the Spike. Jujuboside B, Linoleic acid, and Allantoin are the three ligands that have interaction with all three subunits identified by rigid-docking; however, Jujuboside B is the only ligand that retains the interaction between all the subunits post-MD. Glycyrrhizin, which during rigid docking interacted with only one subunit, interacts with all three subunits on the reorganization of the binding site during MD simulation. The reorganization later in time may lead to further stabilization of the binding as evidenced by the Aff_{pseudo} value of – 16.70. Therefore, Jujuboside B and Glycyrrhizin are expected to have a high Spike inhibition efficiency. Looking at Curcumin, it is the only ligand having interaction with two subunits which dynamically changed interaction with subunits during the MD. This indicates that the curcumin binding site is close to the trimer interface and may provide stabilization to the trimer state in a dynamic fashion. Looking at Caffeine and Glucolepidiins which were interacting with two Spike subunits during the rigid-docking, that were also preserved post the MD run, we find that the strength of interaction improved substantially through hydrogen bond or pi/alkyl bond. Allantoin and Linoleic acids are the only two cases that lost interaction with one subunit during the MD run but improved upon the binding affinity. Kaempferol has interaction with two subunits and after the MD run was left interacting with only one subunit. Malvone A and Vascine have conserved interaction with one subunit.

A general confirmation of the above observations made can be verified from the trends seen for the change in binding affinities for each of the ligands based on their interactions across the number of subunits (Table 1, last row). The higher number of subunits a ligand interacts with, the more it appears to gain in strength of affinity after the MD simulation. In these cases, both Aff_{MD} / Aff_{pseudo} can be used for the purpose because they are essentially the same simulation, with the difference of motion being local. This has been verified by plotting the RMSF, RMSD, R_G, and SASA plots for both box-centered and PBC-translated structures of Spike, which are identical in their traces (Figure 2).

3.4 Comparison of structural dynamics features of ligand-bound complex against the spike receptor

The difference in structural behavior of the complex and the receptor was assessed using the fluctuation graphs (Figure 2). The difference in the RMSD is minimal (Figure 2A) and mostly bound within |0.05| nm. Considering the large size of the Spike protein, the small value

indicates that the overall motions of the receptor are broadly conserved, except for the Jujuboside B bound complex, which shows a distinct R_G trajectory (Figure 2B) that is more compact than the others. This observation that the MD difference between the receptor and ligand complex is minor is also confirmed when RMSF (Figure 2C) and the ASA (Figure 2D) plots are analyzed.

Table 1: Comparative study of protein-ligand interaction

Parameters	After protein-ligand docking	After molecular dynamics
Caffeine (CID 2519) Aff_{dock}: -6.5 Aff_{MD}: -10.7 Aff_{pseudo}: -6.3 A 4 1 1 1 B C 8 1 1 A 7 1 8 B C 8 1 2	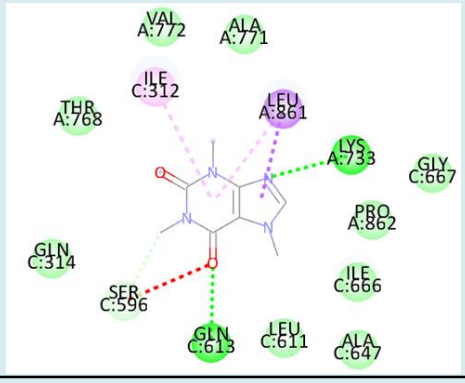	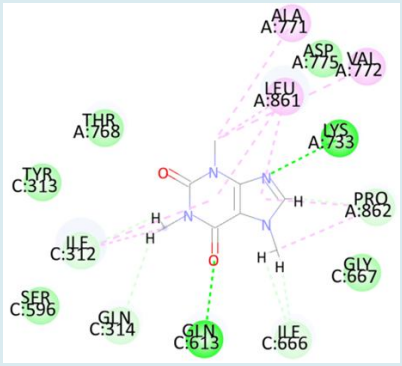
Curcumin (CID 969516) Aff_{dock}: -8.82 Aff_{MD}: -17.9 Aff_{pseudo}: -12.9 A 11 3 1 B C 11 1 3 A B 4 2 1 2 C 5 1 3	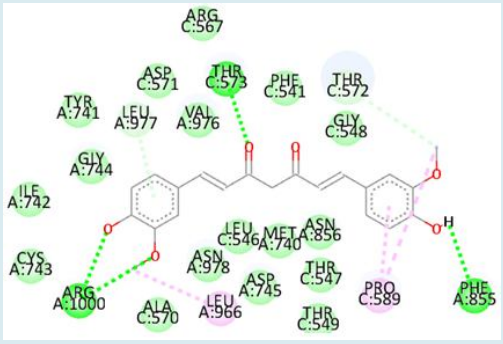	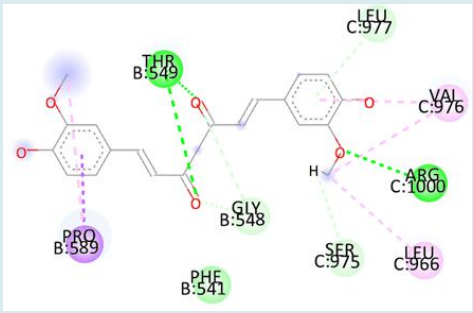
Glycyrrhizin (CID: 14982) Aff_{dock}: -10.23 Aff_{MD}: -8.6 Aff_{pseudo}: -16.70 A 14 3 B C A 1 1 B 4 1 C 1 1	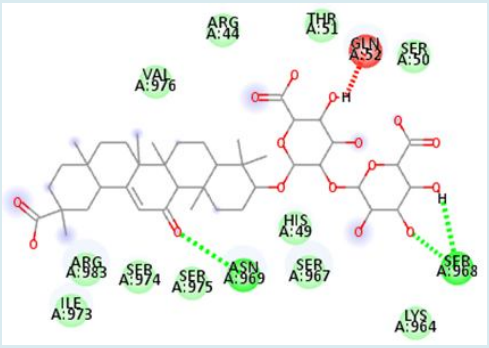	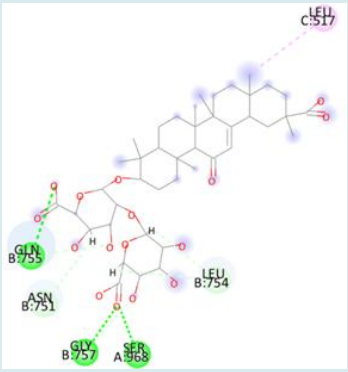
Jujuboside B(24721031) Aff_{dock}:-11.6 Aff_{MD}: -25.5 Aff_{pseudo}: -22.2 A 6 B 9 2 2 C 12 2 A 3 1 B 8 1 3 C 13 3 4	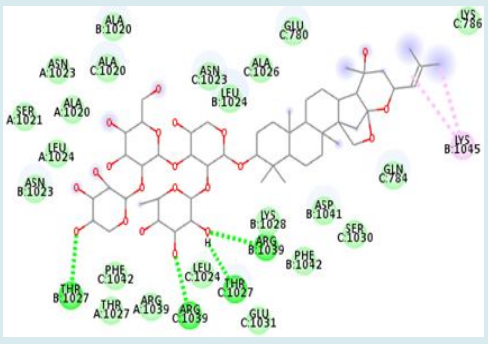	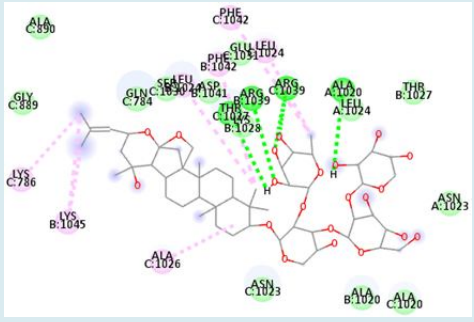

Glucolepidiin (656547) Aff_{dock}: -7.45 Aff_{MD}: -13.3 Aff_{pseudo}: -18.8 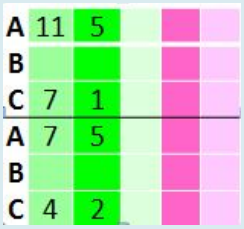	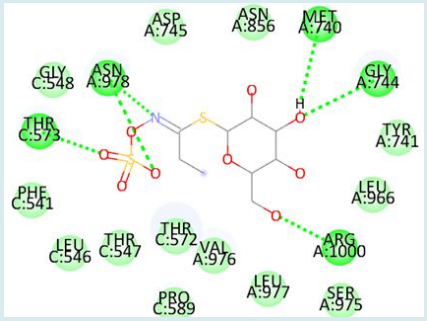	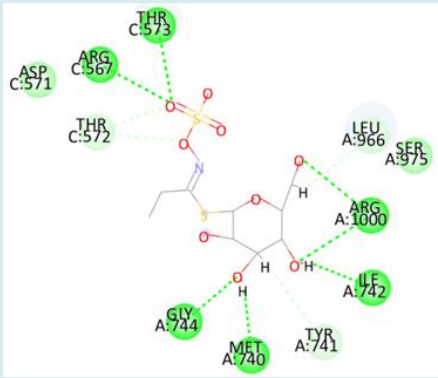
Linoleic acid (CID 5280450) Aff_{dock}: -6.26 Aff_{MD}: -7.5 Aff_{pseudo}: -10.0 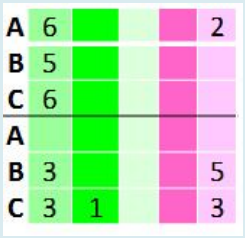	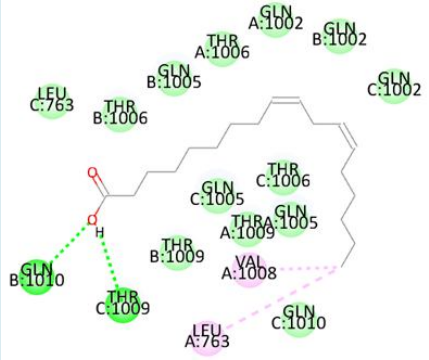	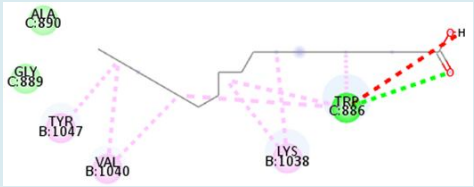
Kaempferol (CID 5280863) Aff_{dock}:: -8.5 Aff_{MD}: -12.3 Aff_{pseudo}: -22.6 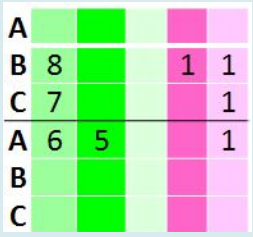	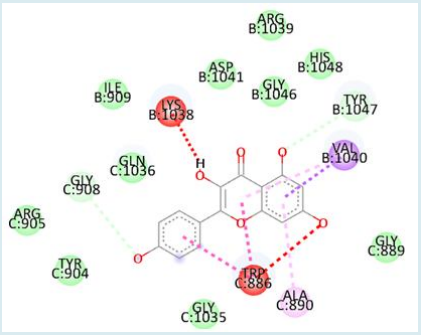	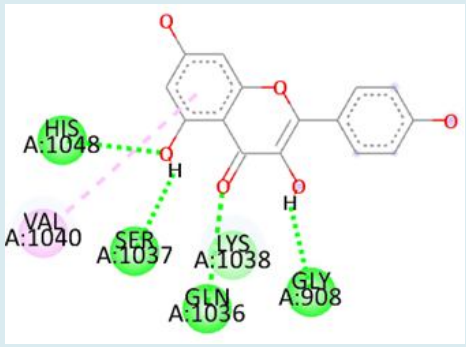
Malvone A(CID 135542082) Aff_{dock}: -7.6 Aff_{MD}: -6.7 Aff_{pseudo}: -8.48 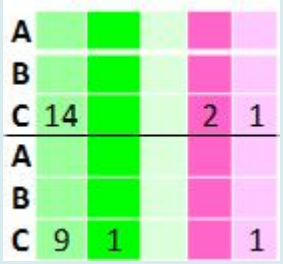	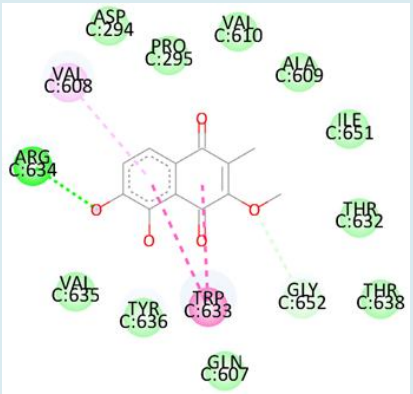	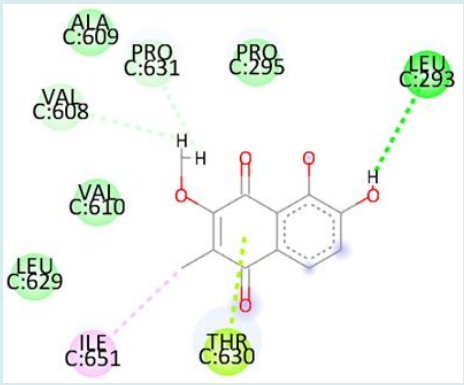

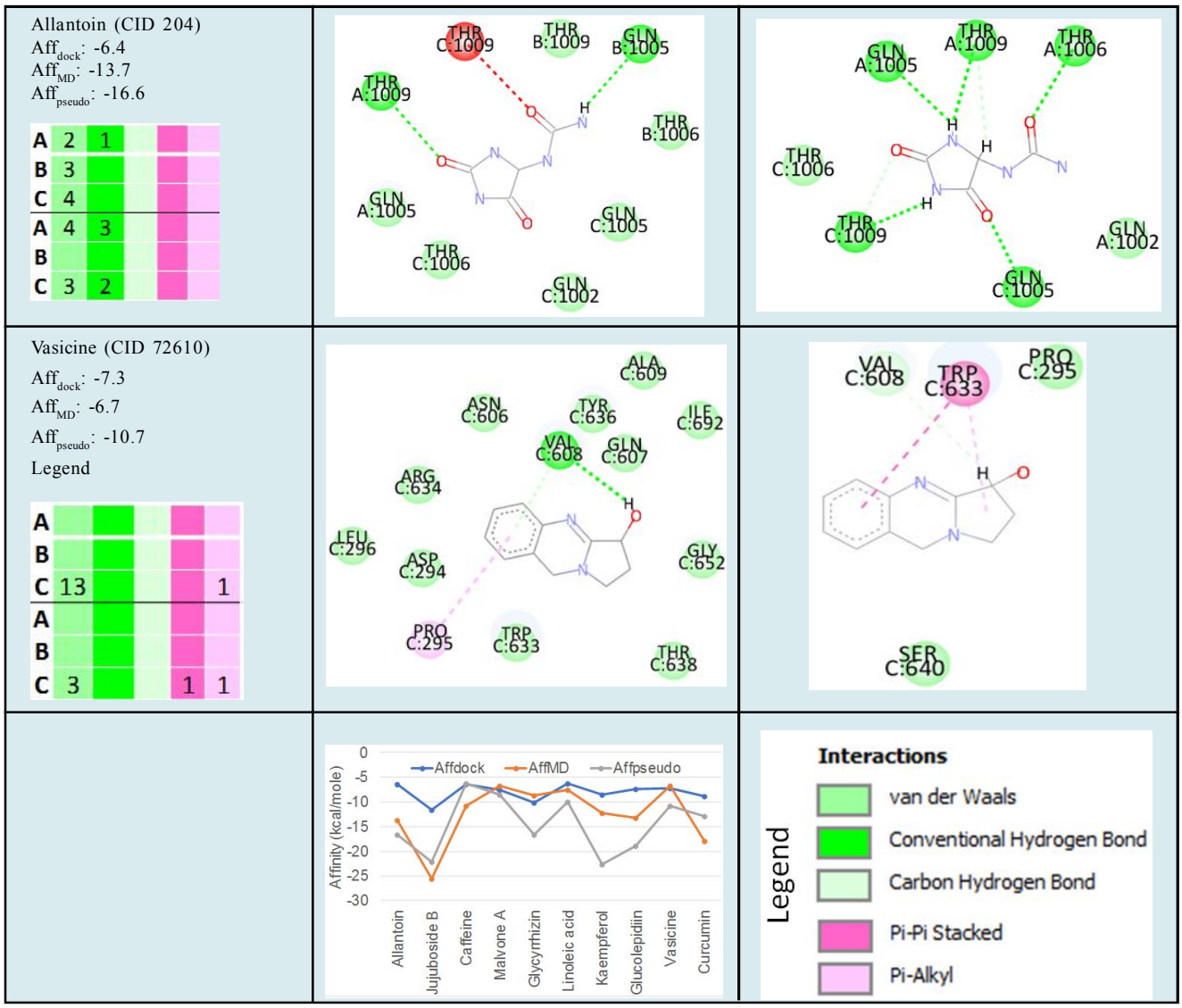

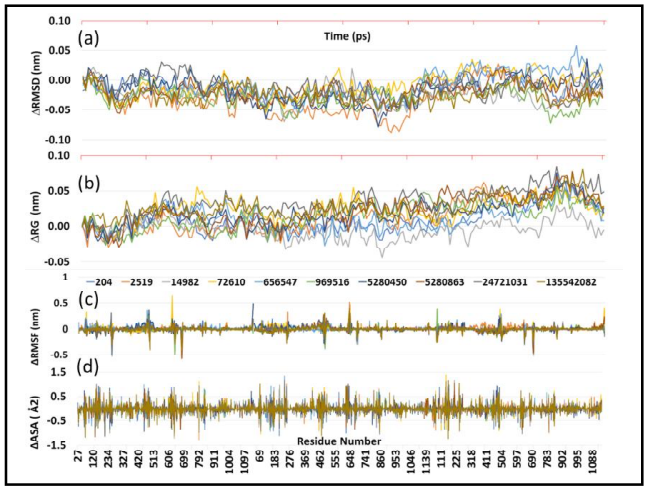

Figure 2: Plots comparing different structural dynamics features for the ligand-bound Spike complex and the Spike-only recep-tor. The ligands are denoted by their compound identifiers (CID). (A) Differences are calculated for the Root Mean Square Deviation (RMSD), (B) Radius of Gyration (R_G), (C) Root Mean Square Fluctuation (RMSF), and (D) Accessible Surface Area (ASA). Note that except for Jujuboside B (CID 20721031) showing a distinct R_G trace (in B) for about 10 ns in the later half of the trajectory, there are no other segments of the plots in the figure where there is a distinct color segregation indicating a unique structural behavior of the complex due to ligand binding. The traces are identical to the trajectories obtained from the pseudo setup created from the PBC definition (Figure 1B).

4. Discussion

The ligand binding prediction is routinely done using rigid-body docking followed by MD to verify the stability of the affinity predictions. We have also used the same strategy in the current study, except that we have additionally used a pseudo-setup to run molecular dynamics. The motivation for running this setup was to compensate for the timescale of the simulation runs in our study,

which are on the shorter side (20 ns). Spike is a large protein of over 1200 x 3 = 3600 residues that take significant computational resources. Using the PBC to setup the problem in another way allowed us to explore the ligand affinity space, as evidencedby the different Aff_{MD} andAff_{pseudo} values, which indicates that our experiments were fruitful, given that identical RMSD, ASA, RMSF, and R_G parameters were obtained.

The interpretation of affinity values by their magnitude is not entirely correct if not done keeping the context in mind. A high-affinity value for Jujuboside B and Kaempferol cannot be interpreted in the same way, the former has Aff_{pseudo}: of – 22.2, while the latter has – 22.6 kcal/mole, but Jujuboside B extensively interacts with all three subunits, whereas Kaempherol does not. The different effect on altered Spike stability is seen from Figure 2B plot for R_G from Jujuboside B, where the trace is in the negative "R_G region.

Not all sites in a homotrimeric protein may have a conducive shape and size to allow simultaneous interaction with all the subunits. However, those ligands such as Curcumin and Glycyrrhizin which are initially interacting with one or two subunits close to the trimer interface can flip the interaction-subunit partner dynamically offering an equally efficient way to inhibit the Spike proteins. The homodimeric setup and the symmetry of the receptor structure offer this unique opportunity to exchange interaction, which is also a plausible way of inhibition that can happen in the physiological condition.

5. Conclusion

Bioactive compounds offer unique possibilities of inhibiting the Spike protein, which is known to be a major determinant of COVID-19. Structural and dynamics studies from this work suggest that this inhibition is reinforced more firmly in the fluctuating environment of the molecule as encapsulated by molecular dynamics simulations. Those ligands which are located in the grooves near the Spike trimer interface are better placed for effective inhibition compared to sites that are limited to one subunit alone. In this context, Jujuboside B and Glycyrrhizin are the top two compounds predicted to be the most effective, while Vasicine is deemed to be least effective at its predicted docking site.

Funding

The authors extend their appreciation to the Deputyship of Research and Innovation in Saudi Arabia for funding this research work through project number IFP2021-090.

Acknowledgments

The authors are thankful to the Deanship of Scientific Research, Shaqra University, Saudi Arabia.

Conflict of interest

The authors declare no conflicts of interest relevant to this article.

References

Woodbridge, Y.; Amit, S.; Huppert, A. and Kopelman, N. M. (2022). Viral load dynamics of SARS-CoV-2 Delta and Omicron variants following multiple vaccine doses and previous infection. Nature Communications, **13**(1):6706.

Focosi D. (2023). From Co-Administration to Co-Formulation: The race for new vaccines against COVID-19 and other respiratory viruses. Vaccines, **11**(1):109.

Chavda, V. P.;Baviskar, K. P.; Vaghela, D. A.; Raut, S. S. and Bedse, A. P. (2023). Nasal sprays for treating COVID-19: A scientific note. pharmacological reports: pp:1-17. Advance Online Publication.

Tao, K.; Tzou, P. L.; Nouhin, J.; Bonilla, H.; Jagannathan, P. and Shafer, R. W. (2021). SARS-CoV-2 antiviral therapy. Clinical Microbiology Reviews, **34**(4):e0010921.

Sarkar, L.; Oko, L.; Gupta, S.; Bubak, A. N.; Das, B.; Gupta, P.;Safiriyu, A. A.; Singhal, C.; Neogi, U.; Bloom, D.; Banerjee, A.; Mahalingam, R.; Cohrs, R. J.; Koval, M.; Shindler, K. S.; Pal, D.; Nagel, M. and Sarma, J. D. (2022). *Azadirachta indica* A. Juss bark extract and its nimbin isomers restrict α-coronaviral infection and replication. Virology, **569**:13-28.

Hall, S.; Desbrow, B.; Anoopkumar-Dukie, S.; Davey, A. K.; Arora, D.; Mc Dermott, C.; Schubert, M. M.; Perkins, A. V.; Kiefel, M. J. and Grant, G. D. (2015). A review of the bioactivity of coffee, caffeine and key coffee constituents on inflammatory responses linked to depression. Food Research International (Ottawa, Ont.), **76**(Pt 3):626-636.

Chainani-Wu N. (2003). Safety and anti-inflammatory activity of curcumin: a component of turmeric (*Curcuma longa*). Journal of Alternative and Complementary Medicine (New York, N.Y.), **9**(1): 161-168.

Luo, P.; Liu, D. and Li, J. (2020). Pharmacological perspective: Glycyrrhizin may be an efficacious therapeutic agent for COVID-19. International Journal of Antimicrobial Agents, **55**(6):105995.

Seo, E. J.; Lee, S. Y.; Kang, S. S. and Jung, Y. S. (2013). *Zizyphus jujuba* and its active component jujuboside B inhibit platelet aggregation. Phytotherapy Research PTR, **27**(6):829-834.

Ninave, P. B. and Patil, S. D. (2019). Antiasthmatic potential of *Zizyphus jujuba* Mill and Jujuboside B. : Possible role in the treatment of asthma. Respiratory Physiology and Neurobiology, **260**:28-36.

Zhao, Y.; Zhang, X.; Li, J.;Bian, Y.; Sheng, M.; Liu, B.; Fu, Z.; Zhang, Y. and Yang, B. (2016). Jujuboside B reduces vascular tension by increasing Ca^{2+} influx and activating endothelial nitric oxide synthase. PloS One, **11**(2):e0149386.

Romeo, L.; Iori, R.; Rollin, P.; Bramanti, P. and Mazzon, E. (2018). Isothiocyanates: An overview of their antimicrobial activity against human infections. Molecules (Basel, Switzerland), **23**(3):624.

Jandacek R. J. (2017). Linoleic acid: A nutritional quandary. Healthcare (Basel, Switzerland), **5**(2):25.

Devi, K. P.; Malar, D. S.; Nabavi, S. F.; Sureda, A.; Xiao, J.; Nabavi, S. M. and Daglia, M. (2015). Kaempferol and inflammation: From chemistry to medicine. Pharmacological Research, **99**:1-10.

Mousavi, S. M.; Hashemi, S. A.; Behbudi, G.; Mazraedoost, S.; Omidifar, N.; Gholami, A.; Chiang, W. H.; Babapoor, A. and Pynadathu Rumjit, N. (2021). A review on health benefits of *Malva sylvestris* L. nutritional compounds for metabolites, antioxidants, and anti-Inflammatory, anticancer, and antimicrobial applications. Evidence-based Complementary and Alternative Medicine: eCAM, 2021:5548404.

Araújo, L. U.; Grabe-Guimarães, A.; Mosqueira, V. C.; Carneiro, C. M. and Silva-Barcellos, N. M. (2010). Profile of wound healing process induced by allantoin. Acta Cirurgicabrasileira, **25**(5):460-466.

Gulati, K.; Rai, N.; Chaudhary, S. and Ray, A. (2016). Nutraceuticals in Respiratory disorders, Editor(s): Ramesh C. Gupta, Nutraceuticals, Academic Press, pp:75-86.

Farag, M.; Pathan, A. and Aldoj, N. (2022). Molecular docking analysis of ten plant products for the inhibition of spike glycoprotein and prospective use as anti-COVID compounds. Ann. Phytomed., **11**(2):302-308.

Pal D. (2021). Spike protein fusion loop controls SARS-CoV-2 fusogenicity and infectivity. Journal of Structural Biology, **213**(2):107713.

Walls, A. C.; Park, Y. J.; Tortorici, M. A.; Wall, A.; Mc Guire, A. T. and Veesler, D. (2020). Structure, function, and antigenicity of the SARS-CoV-2 Spike glycoprotein. Cell, **181**(2):281-292.e6.

Trott, O. and Olson, A. J. (2010). AutoDock Vina: Improving the speed and accuracy of docking with a new scoring function, efficient optimization, and multithreading. Journal of Computational Chemistry, **31**(2):455-461.

Abraham, M. J.; Murtola, T.; Schulz, R.; Páll, S.; Smith, J. C.; Hess, B. and Lindahl, E. (2015). GROMACS: High performance molecular simulations through Multi-Level parallelism from laptops to super computers. Softwar, eX,1-2,19-25.

Huang, J. and MacKerell, A.D. Jr. (2013). CHARMM36 all-atom additive protein force field: Validation based on comparison to NMR data. Journal of Computational Chemistry, **34**(25):2135-2145.

Bussi, G.;Donadio, D. and Parrinello, M. (2007). Canonical sampling through velocity rescaling. The Journal of Chemical Physics, **126**(1): 014101.

Parrinello, M. and Rahman, A. (1981). Polymorphic transitions in single crystals: A new molecular dynamics method. Journal of Applied Physics, **52**(12):7182-7190.

Vanommeslaeghe, K. and MacKerell, A. D., Jr (2012). Automation of the CHARMM general force field (CGenFF) I: Bond perception and atom typing. Journal of Chemical Information and Modeling, **52**(12):3144-3154.

Vanommeslaeghe, K., Raman, E. P. and MacKerell, A. D., Jr (2012). Automation of the CHARMM general force field (CGenFF) II: Assignment of bonded parameters and partial atomic charges. Journal of Chemical Information and Modeling, **52**(12):3155-3168.

Citation **Medhat Farag, Aslam Pathan and Nawaf Aldoij (2023). Interaction between anti-COVID compounds across spike protein subunits influences their inhibitionpotential. Ann. Phytomed., 12(1):251-258. http://dx.doi.org/10.54085/ap.2023.12.1.27.**